

Two-Photon Exclusive Processes in Quantum Chromodynamics*

STANLEY J. BRODSKY

*Stanford Linear Accelerator Center
Stanford University, Stanford, California, 94305*

ABSTRACT

QCD predictions for $\gamma\gamma$ annihilation into single mesons, meson pairs, and baryon pairs are reviewed. Two-photon exclusive processes provide the most sensitive and practical measure of the distribution amplitudes, and thus a critical confrontation between QCD and experiment. Both the angular distribution and virtual photon mass dependence of these amplitudes are sensitive to the shapes of the $\phi(x, Q)$. Novel effects involving the production of $qq\bar{q}\bar{q}$ states at threshold are also discussed, and a new method is presented for systematically incorporating higher-order QED corrections in $\gamma\gamma$ reactions.

1. INTRODUCTION

Two-photon processes provide many of the most critical tests of quantum chromodynamics. In contrast to the uncalculability of hadronic structure functions, QCD perturbation theory predicts the shape in x and the magnitude of the photon structure function $F_2^\gamma(x, Q^2)$. Experiments¹ have verified the striking prediction that the evolution of F_2^γ is increasing and linear in $\ln Q^2$.

More generally, inclusive two-photon processes at large transverse momenta are consistent² with the elementary scaling and canonical normalization $N_C \times \sum e_Q^4$ of the cross section predicted by the simplest $\gamma\gamma \rightarrow \bar{q}q$ subprocess - even at transverse momenta as low as 2 to 3 GeV/c.

Given these successes in the inclusive domain, it is natural to ask how well two-photon *exclusive* processes can be predicted by the theory. This is especially important in view of the uncertainties in determining at what scale leading twist predictions based on perturbative analyses become reliable.

* Work supported by the Department of Energy, contract DE - AC03 - 76SF00515.

QCD has two essential properties which make calculations of processes at short distance or high momentum transfer tractable and systematic. The critical feature is asymptotic freedom: the effective coupling constant $\alpha_s(Q^2)$ which controls the interactions of quarks and gluons at momentum transfer Q^2 vanishes logarithmically at large Q^2 . Complementary to asymptotic freedom is the existence of factorization theorems for both exclusive and inclusive processes at large momentum transfer. In the case of exclusive processes (in which the kinematics of all the final state hadrons are fixed at large invariant mass), the hadronic amplitude can be represented as the product of a hard-scattering amplitude for the constituent quarks convoluted with the distribution amplitude for each incoming or outgoing hadron.³⁻⁷ Exclusive processes in QCD are thus interesting because they provide a window for viewing the wavefunctions of hadrons in terms of their quark and gluon degrees of freedom. The essential non-perturbative input is the hadron “distribution amplitude” $\phi(x, Q)$ which describe the longitudinal momentum distribution of the quarks in the valence, lowest-particle-number Fock state.

The distribution amplitude contains all of the bound-state dynamics and specifies the momentum distribution of the quarks in the hadron.³ The hard scattering amplitude can be calculated perturbatively as a function of $\alpha_s(Q^2)$. The analysis can be applied to form factors, exclusive photon-photon reactions, photoproduction, fixed-angle scattering, *etc.* In the case of the simplest processes, $\gamma\gamma \rightarrow M\bar{M}$ and the meson form factors, rigorous all-orders proofs can be given.³⁻⁸

The wavefunction $\psi_V(x, k_\perp)$ is defined as the valence Fock state wavefunction defined at equal light-cone time in light-cone gauge where $x = (k^0 + k^z)/(p^0 + p^z)$. Then

$$\phi(x, Q) = \int d^2 k_\perp \theta(Q^2 - k_\perp^2) \psi_V(x, k_\perp);$$

i.e., $\phi(x, Q)$ is the probability amplitude to find the quark and antiquark in the meson (or three quarks in a baryon) collinear up to the transverse momentum scale Q .

More generally, the distribution amplitude can be defined as a gauge-invariant matrix-element product of quark fields evaluated between the QCD vacuum and the hadron state. At large Q^2 one can use an operator product expansion⁷ or an evolution equation³ to determine $\phi(x, Q)$ from an initial value determined by non-perturbative input. To leading order in α_s the eigensolutions and eigenvalues (anomalous dimensions) are specified by conformal symmetry.⁹ In higher orders explicit calculations of the evolution equation kernel show that conformal symmetry is broken in QCD even if the β function is chosen to be zero (by fixing the number of flavors). The origin of this anomaly is not understood.

The central unknown in the QCD predictions at this time is the composition of the hadrons in terms of their quark and gluon quanta. Recently, several im-

portant tools have been developed which allow specific predictions for the hadron wave functions. A primary tool is the use of light-cone quantization to construct a consistent relativistic Fock state basis for the hadrons and their observables in terms of quark and gluon quanta. The distribution amplitudes and the structure functions are defined directly in terms of these light-cone wave functions.³ The form factor of a hadron can be computed exactly in terms of a convolution of initial and final light-cone Fock state wave functions.¹⁰

The actual computation of distribution amplitudes and structure functions in QCD is now just at the beginning stages. Structure functions are very complex objects since a complete sum over squares of all hadron Fock amplitudes is required. The distribution amplitude only requires knowledge of the lowest valence Fock amplitude. Several methods are now being explored:

(1). In simple models, explicit solutions to the Bethe Salpeter equation (in ladder approximation) are known, based on the Wick-Cutkosky analysis. The distribution amplitude can be determined for these model theories by evaluating the solutions at equal light-cone time $\tau = t + z/c$. The relation of these solutions to that of the Weinberg equation is discussed in ref. 11.

(2). By imposing periodic boundary conditions in the light-cone variable $z^- = z - ct$, one can reduce the problem of solving field theories in one-space and one-time dimensions to the problem of diagonalizing a finite-matrix representation of the light-cone Hamiltonian.¹² The eigenvalues and eigenfunctions of H_{LC} correspond to the spectrum and Fock-state wavefunctions of the theory. Thus far the discretized light-cone quantization (DLCQ) analysis has been carried out for Yukawa interactions and QED for massless and massive fermions in 1+1 dimensions. The distribution amplitude for the lowest state as a function of coupling constant can then be obtained. We are currently extending the analysis to QCD in 1+1 and 3+1 dimensions.

(3). An important advance has been the numerical evaluation of moments of distribution amplitudes using lattice gauge theory.¹³ The initial results are provocative – suggesting a highly structured oscillating momentum-space valence wave function for the meson. Results for the pion distribution amplitude are shown in fig. 1.

The existence of nodes in a momentum-space amplitude is perhaps suggestive of a bag-like model with sharp boundary conditions. The lattice QCD analysis done by Gottlieb, Kronfeld, and Photiadis is technically complex; in particular, one must judiciously select operator matrix elements which do not contain power-law divergences in the renormalization scale. Limitations in the method are discussed in ref. 13.

(4). The most detailed results and predictions for the hadron distribution amplitudes have been obtained using the ITEP QCD sum rule analysis. Candi-

date hadronic wavefunctions have been derived⁵ using this method which relate the first few x -moments of the meson and baryon distribution amplitudes to the values of the QCD vacuum condensates $\langle 0 | G_{\mu\nu}^2 | 0 \rangle$ and $\langle 0 | m\bar{\psi}\psi | 0 \rangle$. In the pion case, predictions for the normalization of the weak decay constant and the sign and magnitude of the pion form factor for Q^2 above 2 GeV^2 are consistent with experiment. The distribution amplitude for pions and rho-mesons with helicity zero is predicted to be double-humped, with a local minimum at $x = \frac{1}{2}$ (see fig. 1).

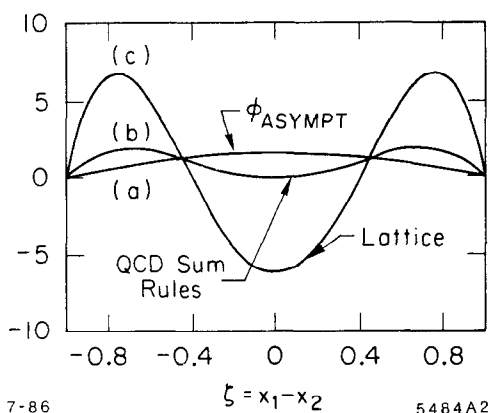


Fig. 1. The pion distribution amplitude calculated in lattice gauge theory (ref. 13) and QCD sum rules (ref. 5). The asymptotic solution to the QCD evolution equation $\phi(x, Q)_{asympt} = x_1 x_2$ is shown for comparison.

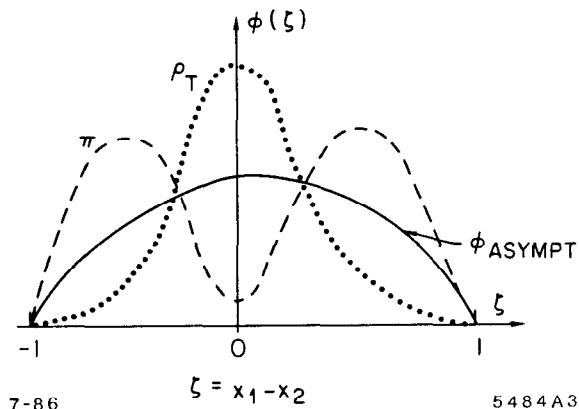


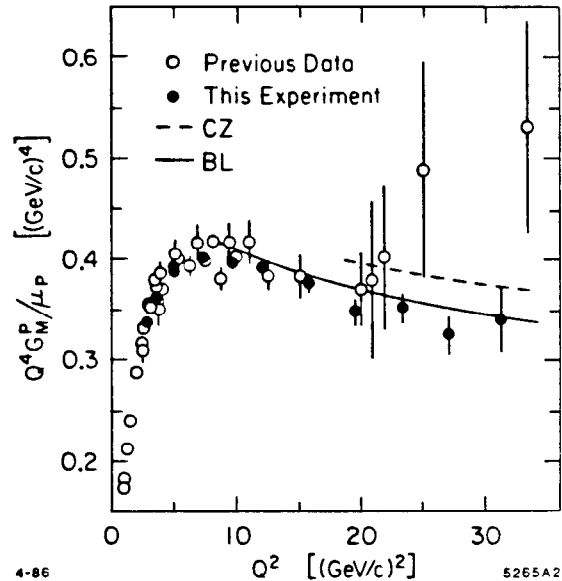
Fig. 2. The pion and transversely-polarized ρ_T distribution amplitudes determined from QCD sum rules (ref. 5).

The distribution amplitude of a ρ -meson with helicity ± 1 is, however, peaked at equal momentum (see fig. 2). This implies a strong dependence of the $\gamma\gamma \rightarrow \rho\rho$ amplitude on a non-perturbative vacuum condensate effect in the ρ wavefunction. In analogy one also expects that the Δ distribution amplitude has a very different shape for helicity $S_z = \frac{3}{2}$ and $S_z = \frac{1}{2}$ states. (This dependence could have a striking effect on the relative normalization of the $\Delta\bar{\Delta}$ and $p\bar{p}$ production cross sections and could very possibly diminish the ratio of 60 predicted by Farrar, Maina, and Neri¹⁴ the basis of symmetric helicity-independent nucleon and isobar wavefunctions.)

A particularly important challenge relevant to exclusive processes is the construction of baryon distribution amplitudes. Using the sum rule method, Chernyak and Zhitnitsky⁵ have proposed a model form for the nucleon distribution amplitude which together with the QCD factorization formulae, predict the correct sign and magnitude as well as scaling behavior of the proton and neutron form factors. The resulting form for the nucleon distribution amplitude leads to a number of

non-trivial predictions: the sign and magnitude of $G_M^P(Q^2)$ at high Q^2 , the ratio G_{M_p}/G_{M_n} and the normalization of $\psi \rightarrow p\bar{p}$ are all correctly determined (see fig. 3). Gari and coworkers¹⁵ have combined these results with a vector dominance model to predict the proton and neutron magnetic and electric form factors at all Q^2 .

Fig. 3. Comparison of the scaling behavior of the proton magnetic form factor with the theoretical predictions of refs. 3 and 5. The CZ predictions⁵ are normalized in sign and magnitude. The data are from ref. 16.



At this time we shall regard the distribution amplitudes derived by Chernyak and Zhitnitskii as very useful Gedanken forms for making predictions for photon-photon exclusive cross sections. The postulated shapes differ significantly from the SU(6)-symmetric asymptotic solution to the distribution amplitude evolution equation: $\phi \propto x_1 x_2 x_3$, or the weak binding form $\phi \propto \delta(x_1 - \frac{1}{3})\delta(x_2 - \frac{1}{3})$. In particular, the proton quark distribution is strongly skewed: the u-quark with helicity parallel to that of the nucleon carries 65% of the nucleon's momentum. This asymmetry also implies that the hadron scattering amplitude is sensitive to the near-endpoint region of integration as well the dependence of the running coupling constant on the exchanged momentum in the hard scattering amplitude. Another special feature of the QCD sum-rule analysis is the strong sensitivity to the hadron helicity. This effect is induced due to the fact that the coupling of a pair of quarks through gluon exchange to the gluon condensate is strongest when the quark and antiquark spins are antiparallel.

There are a large number of uncertainties involved in applying QCD sum rules as wave function constraints, related to the convergence of the scheme, number of resonances included, neglect of higher order operators, etc. Worse, algebraic errors in the analysis of ref. 5. for the nucleon distribution amplitudes have recently been discovered (by King and Sachrajda¹⁷), although the central feature of strong flavor/spin asymmetry is expected to persist.

The results from both the lattice calculations and QCD sum rules demonstrate that the light quarks are highly relativistic in the bound state. This gives further indication that while non-relativistic potential models are useful for enumerating the spectrum of hadrons (because they express the relevant degrees of freedom), they are not reliable in predicting wave function structure.

In any event, two-photon exclusive processes provide the most sensitive and practical measure of the distribution amplitudes, and thus a critical confrontation between non-perturbative QCD and experiment. Both the angular distribution and virtual photon mass dependence of these amplitudes are sensitive to the shapes of the $\phi(x, Q)$. The results and predictions are discussed in the next section.

2. EXCLUSIVE TWO-PHOTON PROCESSES AT HIGH MOMENTUM TRANSFER

The exclusive two-body processes $\gamma\gamma \rightarrow H\bar{H}$ at large $W_{\gamma\gamma}^2 = (q_1 + q_2)^2$ and fixed $\theta_{\text{c.m.}}^{\gamma\gamma}$ provide a particularly important laboratory for testing QCD, since the large momentum-transfer behavior, helicity structure, and often even the absolute normalization can be rigorously predicted.²⁻⁸ Conversely, the angular dependence of $\gamma\gamma \rightarrow H\bar{H}$ cross sections can be used to determine the shape of the hadron distribution amplitudes $\phi_H(x_i, Q)$. The $\gamma_\lambda \gamma_{\lambda'} \rightarrow H\bar{H}$ amplitude can be written as a factorized form⁸ (see figs. 4 and 5):

$$M_{\lambda\lambda'}(W_{\gamma\gamma}, \theta_{\text{c.m.}}) = \int_0^1 [dy_i] \phi_H^*(x_i, Q) \phi_{\bar{H}}^*(y_i, Q) T_{\lambda\lambda'}(x, y; W_{\gamma\gamma}, \theta_{\text{c.m.}}) \quad (1)$$

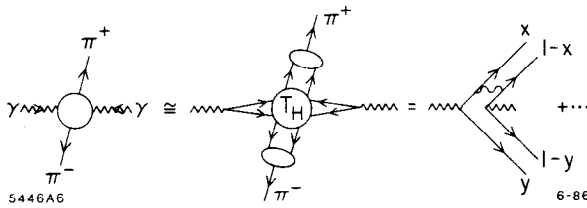


Fig. 4. Application of QCD to two-photon production of meson pairs.

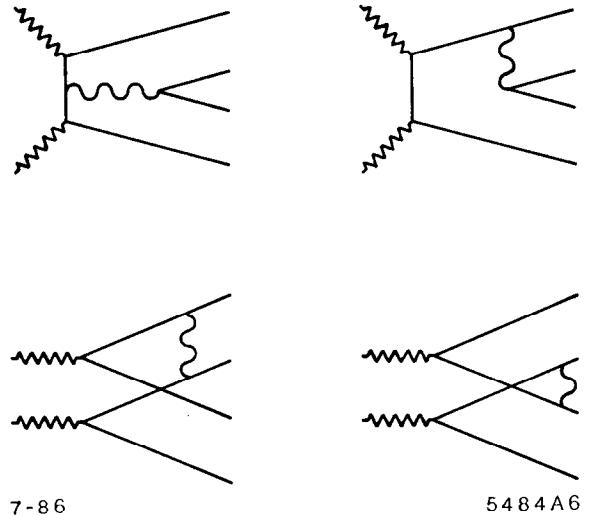


Fig. 5. Lowest order QCD contributions to the $\gamma\gamma \rightarrow$ meson pair hard scattering amplitude T_H .

where $T_{\lambda\lambda'}$ is the hard scattering helicity amplitude for scattering the clusters of valence quarks in each hadron. $T_{\lambda\lambda'}$ can be computed in perturbation theory and scales according to dimensional counting rules:¹⁸ to leading order $T \propto \alpha(\alpha_s/W_{\gamma\gamma}^2)^{1,2}$ and $d\sigma/dt \sim W_{\gamma\gamma}^{-4,-6} f(\theta_{c.m.})$ for meson and baryon pairs, respectively. Lowest order predictions for pseudo-scalar and vector-meson pairs for each helicity amplitude are given in ref. 8 (see fig. 6). The helicities of the hadron pairs are predicted to be equal and opposite to leading order in $1/W^2$. The QCD predictions have now been extended to mesons containing $|gg\rangle$ Fock states by Atkinson, Sucher and Tsokos,²⁰ to $\gamma\gamma \rightarrow p\bar{p}$ and to all $B\bar{B}$ octet and decouplet states by Farrar, Maina and Neri,¹⁴ and Gunion, Millers, and Sparks.²¹ (An earlier calculation by Damgaard²² was apparently erroneous).

A start has now been made to systematically calculate the higher order QCD corrections to the $\gamma\gamma \rightarrow H\bar{H}$ amplitudes. The one-loop corrections to the hard scattering amplitude for meson pairs has been calculated by Nizic²³ (see fig. 7). The simplified asymptotic form of the distribution amplitude was used for illustration. The complete calculation to this order will require the corresponding order α_s corrections to the distribution amplitude.

The basic gauge-invariant measure of a hadron's wavefunction is the distribution amplitude $\phi_H(x_i, Q)$. Using the factorization theorem for exclusive scattering amplitudes, one can show that $\phi_H(x_i, Q)$ is the only non-perturbative input required to normalize and compute any exclusive hadronic scattering processes in QCD at high momentum transfer. As we have discussed in the introduction, one can hope to actually calculate distribution amplitudes from first principles in QCD, e.g. by solving the QCD light-cone equation of motion^{2,12} or from numerical constraints obtained from lattice gauge theory.¹³

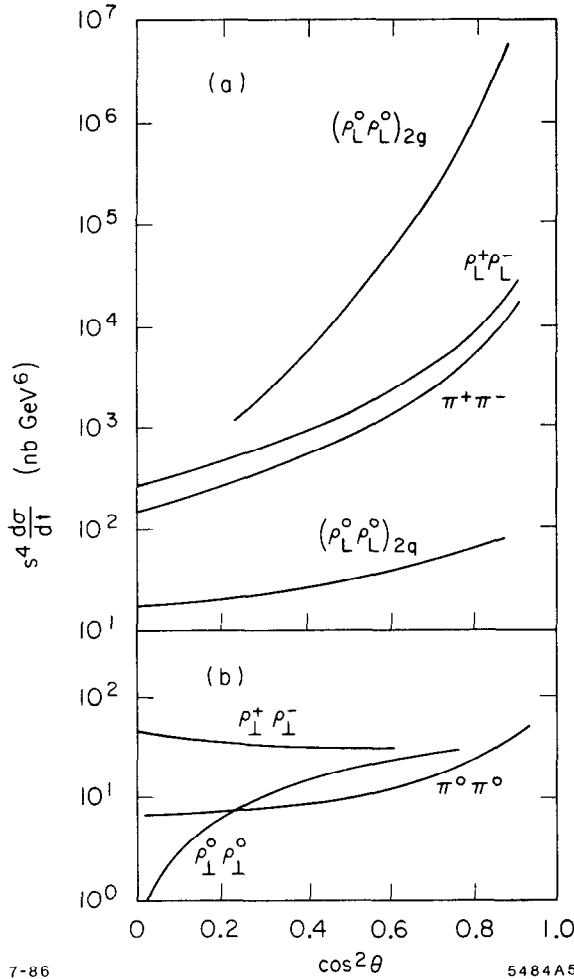
The normalization and angular dependence of the leading order $\gamma\gamma \rightarrow \pi^+\pi^-$ predictions turn out to be insensitive to the precise form of the pion distribution amplitude since the results⁸ can be written directly in terms of the pion form factor taken from experiment. The reason for this is that, for meson distribution amplitudes which are symmetric in x and $(1-x)$, the same quantity

$$\int_0^1 dx \frac{\phi_\pi(x, Q)}{(1-x)} \quad (2)$$

controls the x -integration for both $F_\pi(Q^2)$ and to high accuracy $M(\gamma\gamma \rightarrow \pi^+\pi^-)$. Thus for charged pion pairs we find the relation:

$$\frac{\frac{d\sigma}{dt}(\gamma\gamma \rightarrow \pi^+\pi^-)}{\frac{d\sigma}{dt}(\gamma\gamma \rightarrow \mu^+\mu^-)} \cong \frac{4|F_\pi(s)|^2}{1 - \cos^4 \theta_{cm}} \quad (3)$$

Note that in the case of charged kaon pairs, the asymmetry of the distribution amplitude may give a small correction to this relation.

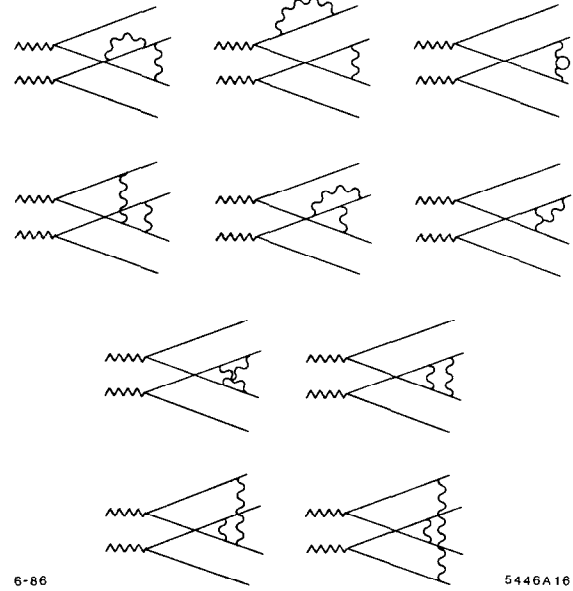


7-86

$\cos^2 \theta$

5484A5

Fig. 6. QCD predictions for the θ_{CM} dependence of meson pair production in $\gamma\gamma$ collisions (from refs. 8 and 19). The zero helicity $\rho^0\rho^0$ cross section is enhanced in the forward direction by multigluon exchange (ref. 19).



6-86

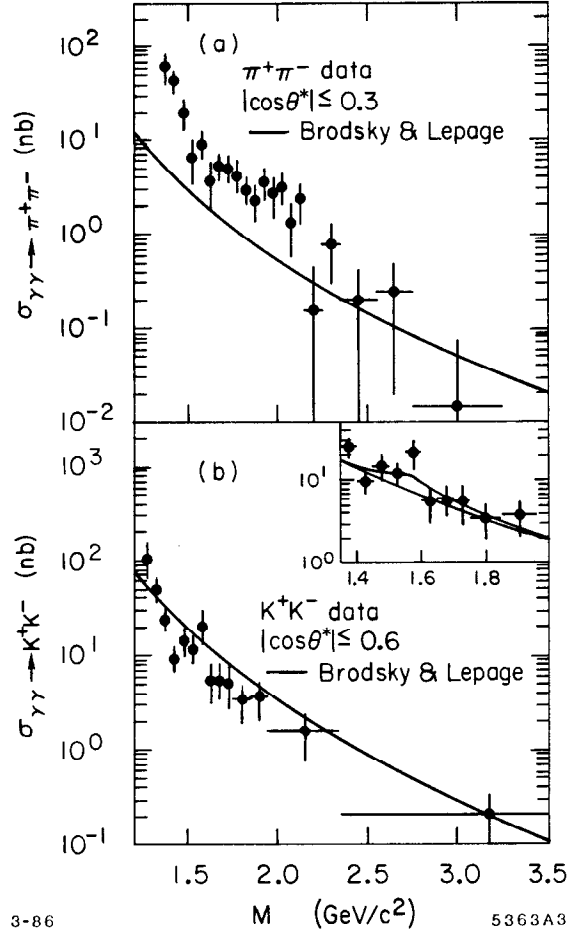
5446A16

Fig. 7. Next to leading perturbative contribution to T_H for the process $\gamma\gamma \rightarrow MM$ calculated by Nizic.²³

The scaling behavior, angular behavior, and normalization of Eq. (2.3) are all non-trivial predictions of QCD. Recent Mark II meson pair data²⁴) and PEP4/PEP9 data²⁵ for separated $\pi^+\pi^-$ and K^+K^- production in the range $1.6 < W_{\gamma\gamma} < 3.2$ GeV near 90° are in excellent agreement with the normalization and energy dependence predicted by QCD (see fig. 8). It is clearly very important to measure the full angular structure of the cross sections, particularly $\pi^0\pi^0$, since the $\cos\theta_{CM}$ dependence can be inverted to determine the x-dependence of the pion distribution amplitude.

The onset of scaling at this range of momentum transfer for meson pair

Fig. 8. Comparison of $\gamma\gamma \rightarrow \pi^+\pi^-$ and $\gamma\gamma \rightarrow K^+K^-$ meson pair production data with the parameter free perturbative QCD prediction of ref. 8. The data are from ref. 25.



production is reasonable since the off-shell quark propagators in the diagrams for T_H carry momenta large compared to the relevant QCD scales: quark masses, intrinsic transverse momentum, and $\Lambda_{\text{QCD}}^{\overline{MS}}$. This is contrary to the conclusions of Isgur and Llewellyn Smith²⁶ who had argued that the QCD exclusive scattering formalism could not account (in leading twist) for the normalization and scaling of the pion and nucleon form factors or other exclusive amplitudes at presently available momentum transfer. The applicability of perturbative QCD to baryon processes in the few GeV regime is however still an open question.

An important exclusive process in QCD is the *sideways* Compton process $\gamma\gamma \rightarrow p\bar{p}$. Applying the procedure of ref. 3 we have, to leading order in $1/p_T^2$,

$$\mathcal{M}_{\gamma\gamma \rightarrow p\bar{p}}(p_T^2, \theta_{CM}) = \int_0^1 [dx] \int_0^1 [dy] \phi_{\bar{p}}(x, p_T) T_H(\gamma\gamma \rightarrow qq\bar{q} + \bar{q}q\bar{q}) \phi_p(y, p_T)$$

where $\phi_p(x, p_T)$ is the antiproton distribution amplitude and $T_H \sim \alpha_s^2(p_T^2)/(p_T^2)$ gives the scaling behavior of the minimally connected tree graph amplitude for

two photons annihilating into three quarks and three antiquarks collinear with the final hadron directions (see fig. 9). QCD thus predicts

$$\frac{d\sigma}{d\Omega_{CM}} (\gamma\gamma \rightarrow p\bar{p}) \simeq \frac{\alpha_s^4(p_T^2)}{(p_T^2)^5} f(p_T, \theta_{CM}, \ln p_T^2) .$$

Complete calculations of the tree graph structure (see figs. 5,9) of both $\gamma\gamma \rightarrow M\bar{M}$ and $\gamma\gamma \rightarrow p\bar{p}$ have now been completed.^{15,21} Examples of the predicted angular distributions are shown in figs. 6, 10, and 11.

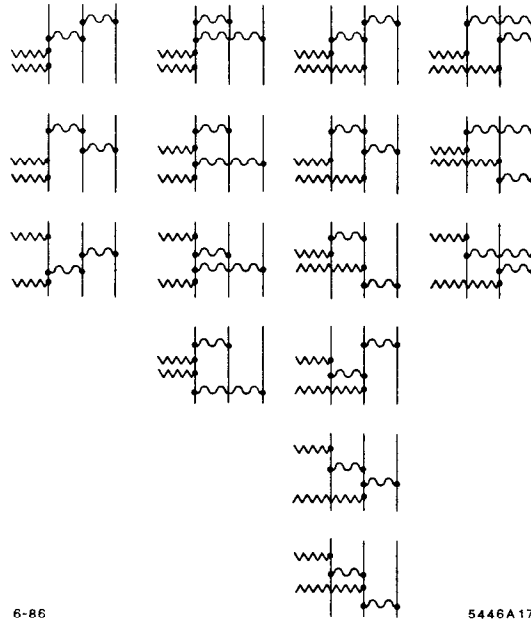
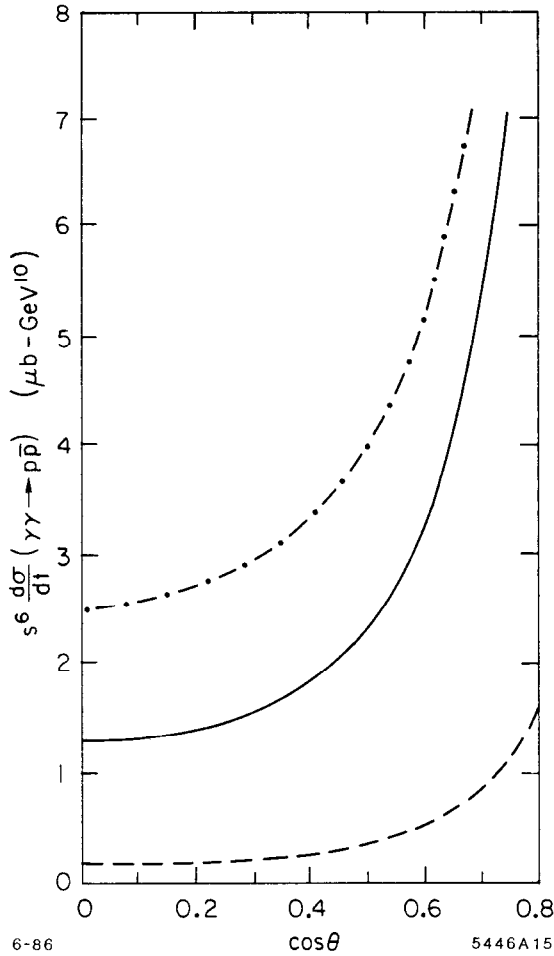


Fig. 9. Leading diagrams for $\gamma + \gamma \rightarrow \bar{p} + p$ calculated in refs. 14 and 21.

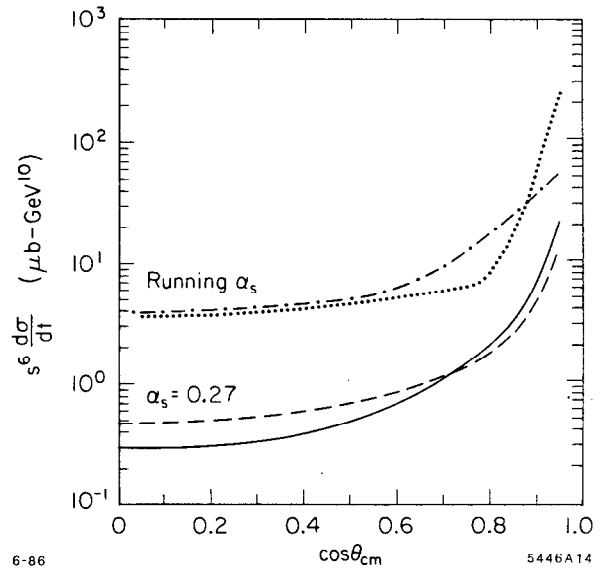
The region of applicability of the leading power-law results is presumed to be set by the scale where $Q^4 G_M(Q^2)$ is roughly constant, *i.e.*: $Q^2 > 3 \text{ GeV}^2$. (See fig. 3.) Preliminary two photon collision measurements²⁷ (for energies too close to the $\bar{p}p$ threshold) are shown in fig. 12. The model form for the proton distribution amplitude proposed by Chernyak and Zhitnitskii⁵ based on QCD sum rules which leads to normalization and sign consistent with the measured proton form factor is used (See fig. 3). As noted above the CZ sum rule analysis has been recently corrected and modified by King and Sachrajda¹⁷ but the final results are not known at this time. It should be noted that unlike meson pair production the QCD predictions for baryons are very sensitive to the form of the running coupling constant and the endpoint behavior of the wavefunctions.

The $\gamma^* \gamma^* \rightarrow \bar{B}B$ and $M\bar{M}$ amplitudes for off-shell photons have now been calculated by Millers and Gunion.²⁸ The results show important sensitivity to the



6-86 5446A15

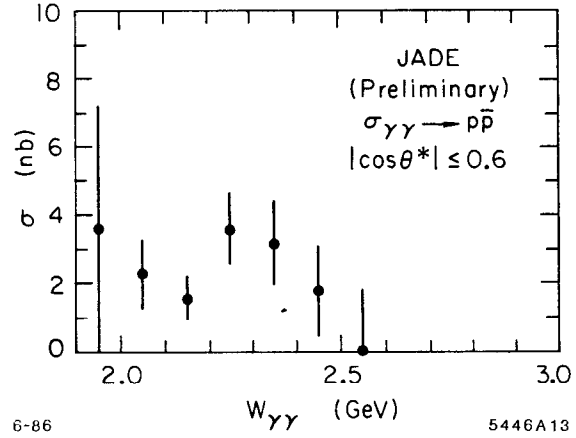
Fig. 10. QCD prediction for the scaling and angular distribution for $\gamma + \gamma \rightarrow \bar{p} + p$ calculated by Farrar et al.¹⁴ The dashed-dot curve corresponds to $\frac{4\Lambda^2}{s} = 0.0016$ and a maximum running coupling constant $\alpha_s^{maz} = 0.8$ The solid curve corresponds to $\frac{4\Lambda^2}{s} = 0.016$ and a maximum running coupling constant $\alpha_s^{maz} = 0.5$ The dashed curve corresponds to a fixed $\alpha_s = 0.3$. The results are very sensitive to the endpoint behavior of the proton distribution amplitude. The CZ form is assumed.



6-86 5446A14

Fig. 11. QCD prediction for the scaling and angular distribution for $\gamma + \gamma \rightarrow \bar{p} + p$ calculated by Gunion, Millers, and Sparks.²¹ CZ distribution amplitudes⁵ are assumed. The solid and running curves are for real photon annihilation. The dashed and dot-dashed curves correspond to one photon spacelike, with $\frac{Q_b^2}{s} = 0.1$.

Fig. 12. Recent preliminary data from JADE²⁶ for $\gamma + \gamma \rightarrow \bar{p} + p$.



form of the respective baryon and meson distribution amplitudes. The consequences of $|gg\rangle$ mixing in singlet mesons in $\gamma\gamma$ processes is discussed in ref. 30.

An essential feature of the QCD predictions for hadron pair production is the fall-off of the cross section at large momentum transfer, reflecting the quark compositeness of the hadrons. One can compare these predictions with the large, rapidly increasing cross sections predicted²⁹ from effective Lagrangian models with *point-like* p , Δ , and γ couplings.

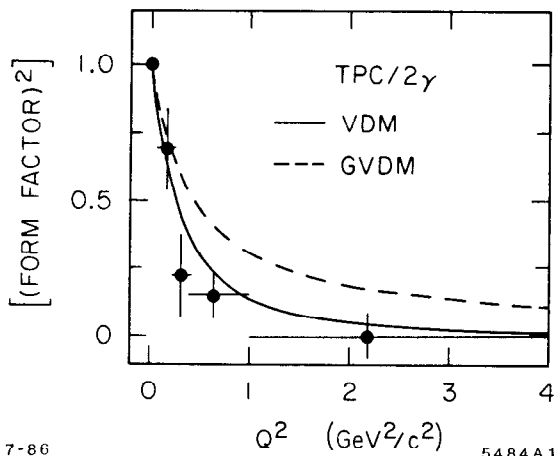
It is important to extend the QCD predictions for $\gamma\gamma \rightarrow H\bar{H}$ to the case of one or two virtual photons, since measurements can be performed with tagged electrons. In fact, for W^2 large and fixed $\theta_{c.m.}$, the q_1^2 and q_2^2 dependence of the $\gamma\gamma \rightarrow H\bar{H}$ amplitude for transversely polarized photons must be minimal.⁸ in QCD since the off-shell quark and gluon propagators in T_H already transfer hard momenta; *i.e.*, the 2γ coupling is effectively local for $|q_1^2|, |q_2^2| \ll p_T^2$.

We also note that photon-photon collisions provide a way to measure the running coupling constant in an exclusive channel, independent of the form of hadronic distribution amplitudes. The photon-meson transition form factors $F_{\gamma \rightarrow M}(Q^2)$, $M = \pi^0, \eta^0, f$, etc. are measurable in tagged $e\gamma \rightarrow e'M$ reactions. QCD predicts^{3,8}

$$\alpha_s(Q^2) = \frac{1}{4\pi} \frac{F_\pi(Q^2)}{Q^2 |F_{\pi\gamma}(Q^2)|^2} \quad (4)$$

where to leading order the pion distribution amplitude enters both numerator and denominator in the same manner. The higher order corrections can be calculated using the methods of refs. 3 and 23. The results of recent measurements of the form factor for single meson production are shown in figs. 13 and 14.

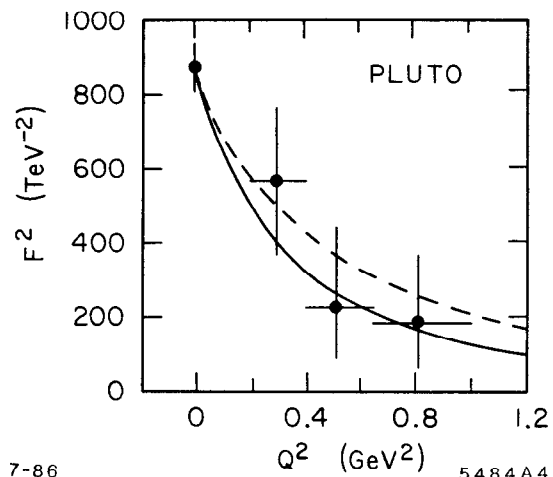
Data from the crossed channel $p\bar{p} \rightarrow \gamma\gamma$ measurable in $p\bar{p}$ collisions at energies up to 9 GeV could clarify the question of whether the perturbative QCD predictions are reliable at moderate momentum transfer.^{26,30} An important check of the QCD predictions can be obtained by combining data from $p\bar{p} \rightarrow \gamma\gamma, \gamma\gamma \rightarrow p\bar{p}$



7-86

5484A1

Fig. 13. The Q^2 dependence of the photon to f^0 transition form factor measured by the TPC/2 γ collaboration at PEP (ref. 32).



7-86

5484A4

Fig. 14. Measurement of the photon to η' transition form factor by the PLUTO collaboration (ref. 33). The solid line is the prediction of a simple ρ pole model, also consistent with QCD expectations. The dashed line is the prediction of a finite size model.

with large angle Compton scattering $\gamma p \rightarrow \gamma p$. This comparison checks in detail the angular dependence and crossing behavior expected from the theory. Furthermore in $p\bar{p}$ collisions one can study timelike photon production into e^+e^- and examine the virtual photon mass dependence of the Compton amplitude. Predictions for the q^2 dependence of the $p\bar{p} \rightarrow \gamma\gamma^*$ amplitude can be obtained by crossing the results of Gunion and Millers.²⁸ The normalization of the $\gamma\gamma \rightarrow p\bar{p}$ amplitude is constrained by the $\psi \rightarrow p\bar{p}$ rate³. The arduous calculation of 280 $\gamma\gamma \rightarrow qq\bar{q}\bar{q}$ diagrams in T_H required for calculating $\gamma\gamma \rightarrow B\bar{B}$ is greatly simplified by using two-component spinor techniques.^{14,21}

In the regime $s \gg p_T^2 \gg \mu^2$ the cross sections for $\gamma\gamma \rightarrow V\bar{V}$ and $\gamma\gamma \rightarrow \gamma V$ can be computed from $n \geq 2$ multiple gluon exchange diagrams by summing a series in $\alpha_s(p_T^2) \ln s/p_T^2$. As shown by Ginzburg, Panfil, and Serbo,¹⁹ the exponentiation of this series leads to large enhancement factors compared to the Born contributions (see fig. 6). The cross sections dominate over the lower-order quark exchange contributions at forward angles. Estimates are also given for $\gamma\gamma \rightarrow Vq\bar{q}$, although in this case soft gluon radiation needs to be included.

3. TWO-PHOTON PRODUCTION PROCESSES AT THRESHOLD

Just as in $e^+e^- \rightarrow H\bar{H}$, the scaling behavior of the Born cross sections can be distorted by resonance production; the leading order predictions are only

be valid well above particle production thresholds and where low relative-velocity final-state corrections become unimportant. [Here we have in mind the QCD analogue of Coulomb interactions between attractive charged particles which, in the non-relativistic regime, give singular distortion factors³² of the form $\zeta/(1-e^{-\zeta})$ where $\zeta = 2\pi\alpha/v$ ($\Rightarrow 8\pi\alpha_s/3v$ in QCD).]

It is important to understand the $\gamma\gamma \rightarrow \pi^+\pi^-$ amplitude in the threshold region since this is the simplest two-body scattering amplitude in QCD. The amplitude is rigorously determined below threshold at $W = 0$ by the low energy theorem for Compton scattering and crossing. The phase of each $\gamma\gamma \rightarrow \pi^+\pi^-$ spherical wave is related by Watson's theorem to the phase of the corresponding $\pi^+\pi^- \rightarrow \pi^+\pi^-$ scattering amplitude. The most detailed predictions employing these constraints, which are obtained by modifying the $\gamma\gamma \rightarrow \pi^+\pi^-$ point-like Born approximation, have been given by Menessier.³³ Data from Pluto³⁴ and DCI³⁶ appear to differ significantly from the model predictions at energies below the f^0 contribution. These results appear to signal a large threshold enhancement in the $\gamma\gamma \rightarrow \pi^+\pi^-$ amplitude, possibly indicating low velocity distortion effects²²⁾ or a new resonance near or below the $\pi^+\pi^-$ threshold. Either possibility has important implications for QCD.

In general, QCD predicts a large array of exotic resonances $q\bar{q}g$, gg , $q\bar{q}q\bar{q}$, $qqq\bar{q}\bar{q}$, etc., which are expected to be prominent in the threshold region of the appropriate $\gamma\gamma$ production channel. In the case of $\gamma\gamma \rightarrow p\bar{p}$, the cross section ($d\sigma/d\cos\theta = 3 \pm 1 \text{ nb}$) measured by TASSO³⁶ in the threshold region $2 < W_{\gamma\gamma} < 2.4 \text{ GeV}$ is roughly 60 times larger than the prediction of Farrar *et al.*,¹⁴ although $\gamma\gamma \rightarrow \Delta^{++}\bar{\Delta}^{++}$ may be close to the predicted normalization. Again this suggests distortions due to resonance production, e.g., $qqq\bar{q}\bar{q}$ baryonium states or strongly helicity-dependent wavefunctions as we have discussed above. The perturbative predictions for $\gamma\gamma \rightarrow B\bar{B}$ would not be expected to become valid unless all of the quark and gluon propagators in T_H are reasonably off-shell, i.e., $W_{\gamma\gamma} \gtrsim 5 \text{ GeV}$ and large θ_{CM} .

Since each photon can independently create a quark pair, the process $\gamma\gamma \rightarrow \bar{Q}Q\bar{Q}Q$ is a natural process in two-photon collisions.^{37,38} At threshold the minimally-connected matrix element is proportional to $e_Q^2\alpha_s(M_Q^2)/M_Q^2$. The Schwinger correction to the four-quark cross section gives a final state Coulomb (soft gluon exchange) correction for each quark pair of the form $\zeta/(1-e^{-\zeta})$ where $\zeta = 2\pi C_F\alpha_s/v_{\text{relative}}$. The final state correction is singular at zero relative velocity, cancelling the phase space suppression. We thus find fairly large threshold $\gamma\gamma$ cross sections of order 1 nb for $s\bar{u}\bar{s}u$ and of order 0.1 nb for $c\bar{u}\bar{c}u$. The above estimates are qualitative but suggestive of the order of magnitude of the cross sections for four-quark continuum and resonance states. A systematic study will be presented in ref. 37. On the other hand, it seems possible to understand the threshold enhancement of $\gamma\gamma \rightarrow \rho^0\rho^0$ from factorization and the behavior of slope

parameters at threshold. This complimentary view is discussed in ref. 38.

The study of resonance production in exclusive two-photon reactions is particularly advantageous because of the variety of new and exotic channels, the absence of complications from spectator hadrons, and the fact that the continuum can be computed or estimated from perturbative QCD. The onset of open charm is particularly interesting since the sum of the exclusive channel cross section should saturate the $\gamma\gamma \rightarrow c\bar{c}$ plus $\gamma\gamma \rightarrow c\bar{c}q\bar{q}$ contributions. The channels with maximal spin and charge such as $\gamma\gamma \rightarrow B_{3/2}(cuu) \bar{B}_{3/2}(\bar{c}u\bar{u})$ are expected to be dominant due to total charge coherence and the counting due to multiple helicity states.

4. SYSTEMATIC APPROACH TO QED/QCD RADIATIVE CORRECTIONS FOR $\gamma\gamma$ PROCESSES

It is not widely known that the standard factorization formula for QCD inclusive processes can be taken over as an elegant and simple method to incorporate QED and QCD radiative corrections for $\gamma\gamma$ processes involving particle production at large transverse momentum. The proof of such results is identical to that applied for proofs^{39,40} of the Drell-Yan formula in gauge field theory. For example the cross section for $e^+e^- \rightarrow \pi^+\pi^-$ (plus any number of collinear photons) has the factorized form⁴¹

$$\frac{d\sigma}{d\Omega dx_a dx_b} = G_{\gamma/e^+}(x_a, Q) G_{\gamma/e^-}(x_b, Q) \frac{d\sigma}{d\Omega}(\gamma\gamma \rightarrow \pi^+\pi^-),$$

where the x_i are the longitudinal light-cone momentum fractions, the G are the structure functions for photons in leptons at the resolution scale $Q = P_{\perp}^{\pi}$, and $\frac{d\sigma}{d\Omega}(\gamma\gamma \rightarrow \pi^+\pi^-)$ is the hard-process cross section which sets the scale. The leading logarithmic corrections from QED radiative corrections to the lepton lines are automatically summed by the evolution equation for the $G_{\gamma/e}(x, Q)$. The beam profile of the collider can be automatically included by defining the initial conditions for the QED structure functions.

Similarly, the cross section for single meson production at large transverse momentum which measures the photon to meson transition form factor has the factorized form

$$\frac{d\sigma}{d\Omega dx_a dx_b} = G_{e^+/e^+}(x_a, Q) G_{\gamma/e^-}(x_b, Q) \frac{d\sigma}{d\Omega}(e^+\gamma \rightarrow Me^+),$$

where $\frac{d\sigma}{d\Omega}(e^+\gamma \rightarrow Me^+)$ is the subprocess cross section predicted to fall as p_T^{-4} in QCD. The structure function $G_{e^+/e^+}(x_a, Q)$ sums the radiative corrections to the positron line. The results of recent measurements of the form factor for single f^0 and η' production are shown in figs. 13 and 14.

The above method has general applicability to e^+e^- annihilation incorporating radiative corrections and the beam profile.^{41,42} For example, consider the inclusive calorimetric production of jet pairs or lepton pairs near the Z^0 peak. If one measures the collinearity angle and jet (hadronic or leptonic) energy with sufficient accuracy, then x_a and x_b are determined. Since the cross section is factorizable, one can separately determine the subprocess cross section $\frac{d\sigma}{d\Omega}(e^+e^- \rightarrow Z^0 \rightarrow e^+e^- \text{ or jet + jet})$ and the beam structure functions (evolved to the Z^0 mass scale) including the machine resolution. Effectively, the QED radiative corrections to the physics cross section are removed.

5. SUMMARY

The apparent agreement of the QCD predictions for $\gamma\gamma \rightarrow \pi^+\pi^-$ and $\gamma\gamma \rightarrow K^+K^-$ with experiment gives support to the applicability of perturbative methods and the hard scattering factorization formalism to meson production at transverse momentum scales as low as 1 to 2 GeV/c. Unlike baryon production processes, the leading twist meson pair predictions are free of complications from end-point contributions or pinch singularities, and are thus first-principle tests of the theory. A complete calculation through next-to-leading contributions in α_s is now underway. Further experimental tests of the angular distribution and helicity dependence of vector meson channels are necessary. In the case of neutral vector meson pairs, the higher order contributions from multi-gluon exchange lead to large forward-peaked diffractive cross sections. One can thus study the perturbative structure of pomeron-exchange channels. We have also emphasized the physics interest in resonant and multi-quark production processes in the threshold region.

Probably the most important aspect of the exclusive $\gamma\gamma$ reactions is the opportunity to measure the shape of the hadron distribution amplitudes, either from the angular distribution of neutral pion pair production or the virtual photon mass dependence of each channels. It should be possible to derive measures of experimental data which determine the distribution amplitude moments. In the case of $\gamma\gamma \rightarrow K\bar{K}$ and $D\bar{D}$, the asymmetry of the distributions due to heavy flavor effects can in principle be studied. We also emphasize the importance of single hadron production $\gamma^*\gamma \rightarrow M^0$ as a measure of the meson distribution amplitudes and a direct determination of the running coupling constant.

Baryon pair production processes are much more problematic since the scale where perturbative predictions become reasonably reliable is probably beyond $p_T \geq 2$ GeV/c. Nevertheless there are many important physics issues to be understood in these relatively simple Compton processes. Complete measurements of nucleon, isobar, and hyperon channels, combined with crossed channel data, is important.

Two-photon exclusive channels can also be studied at the new colliders (SLC, LEP, TRISTAN) with somewhat increased cross sections. The application of in-

clusive factorization formulae (see section 4) simplifies the analysis of the radiative corrections and displays the unity with hadronic collider phenomena. Eventually the effects of $Z^0 - \gamma$ mixing will be measurable, opening up a new range of physics simultaneously involving weak, electromagnetic, and strong interaction physics.

6. ACKNOWLEDGEMENTS

I wish to thank P. Kessler, A. Courau, and M. Froissart for their organization of an excellent meeting.

7. REFERENCES

1. See the reviews of G. Alexander and G. Grunberg, these proceedings.
2. See A. Baecker and J. Stirling, these proceedings.
3. G. P. Lepage and S. J. Brodsky, Phys. Rev. D22, 2157 (1980); G. P. Lepage, S. J. Brodsky, Tao Huang, and P. B. Mackenzie, CLNS-82/522, published in the proceedings of the Banff Summer Institute, 1981.
4. A. H. Mueller, Phys. Rept. 73, 237 (1981).
5. V. L. Chernyak and I. R. Zhitnitskii, Phys. Rept. 112, 1783 (1984). See also Xiao-Duang Xiang, Wang Xin-Nian, and Huang Tao, BIHEP-TH-84, 23 and 29, 1984, and M.J. Lavelle, ICTP-84-85-12; Nucl. Phys. B260, 323 (1985).
6. A. V. Efremov and A. V. Radyushkin, Phys. Lett. 94B, 245 (1980).
7. S. J. Brodsky, Y. Frishman, G. P. Lepage, and C. Sachrajda, Phys. Lett. 91B, 239 (1980).
8. S. J. Brodsky and G.P Lepage, Phys. Rev. D24, 1808 (1981); Phys. Rev. D24, 2848 (1981).
9. S. J. Brodsky, Y. Frishman and G. P. Lepage, Phys. Lett. 167, 347 (1986).
10. S. D. Drell and T. M. Yan, Phys. Rev. Lett. 24, 181 (1970).
11. S. J. Brodsky, C.-R. Ji and M. Sawicki, Phys. Rev. D32, 1530 (1985).
12. H. C. Pauli and S. J. Brodsky, Phys. Rev. D32, 1993 (1985), Phys. Rev. D32, 2001 (1985).
13. S. Gottlieb, A. S. Kronfeld, Phys. Rev. D33, 227-233 (1986); CLNS-85/646, June 1985, p. 22; and the proceedings of the Workshop on Nuclear Chromodynamics, World Scientific, eds. S. J. Brodsky and E. Moniz; A. S. Kronfeld and D. M. Photiadis, Phys. Rev. D31, 2939 (1985).
14. M. Gari and N. G. Stefanis, RUB-TPII-85-16 (Dec. 1985), unpublished.
15. G. R. Farrar, E. Maina and F. Neri, Nucl. Phys. B259, 702 (1985), Err.-ibid. B263, 746 (1986).
16. R. G. Arnold *et al.*, SLAC-PUB-3810, April 1986.

17. I. D. King and C. T. Sachrajda, SHEP-85/86-15, April 1986, p. 36.
18. S. J. Brodsky and G. R. Farrar, Phys. Rev. Lett. 31, 1153 (1973); Phys. Rev. D11, 1309 (1975).
19. I. F. Ginzburg, S. L. Panfil and V.G. Serbo, TF-26-139 (Oct. 1985), unpublished.
20. G. W. Atkinson, J. Sucher and K. Tsokos, Phys. Lett. 137B, 407 (1984).
21. J. F. Gunion, D. Millers and K. Sparks, Phys. Rev. D33, 689 (1986).
22. P. H. Damgaard, Nucl. Phys. B211, 435 (1983).
23. B. Nezcic, Ph.D. Thesis, Cornell University (1985).
24. J. Boyer *et al.*, Phys. Rev. Lett. 56, 207 (1986).
25. TPC/Two Gamma Collaboration (H. Aihara *et al.*), UCR-TPC-86-01, April 1986.
26. N. Isgur and C. H. Llewellyn Smith, Phys. Rev. Lett. 52, 1080 (1984).
27. R. Brandelik *et al.*, Phys. Lett. 108B, 67 (1982). See also the Proceedings of the VIth International Workshop on Two Photon Reactions, Lake Tahoe, CA (1984), edited by R. L. Lander.
28. D. Millers and J. F. Gunion, UCD-86-04, 1986.
29. E. Bagán, A. Bramon and F. Cornet, Barcelona preprint UAB-FT-99 (1983).
30. O. C. Jacob and L. S. Kisslinger, Phys. Rev. Lett. 56, 225 (1986).
31. Further discussion is given in S. J. Brodsky, SLAC-PUB-4010, June 1986.
32. See for example S. J. Brodsky and J. F. Gunion SLAC-PUB-3527, December 1984, published in SLAC Summer Institute, 1984, p. 603.
33. C. Mennessier, Z. Phys. C16, 241 (1983).
34. M. Feindt, these proceedings.
35. A. Falvard, these proceedings
36. U. Karshon, these proceedings, and refs. therein.
37. P. Zerwas, G. Kopp and S. J. Brodsky (in preparation).
38. For a discussion of VDM and amplitude factorization, see G. Alexander, S. J. Brodsky and S. Meshkov.
39. G. T. Bodwin, Phys. Rev. D31, 2616 (1985); G. T. Bodwin, S. J. Brodsky and G. P. Lepage, ANL-HEP-CP-85-32-mc, 1985; presented at the 20th Rencontre de Moriond, Les Arcs, France, March 10-17, 1985.
40. J. C. Collins, D. E. Soper and G. Sterman, Phys. Lett. 134B, 263 (1984).
41. S. J. Brodsky, B. Lynn and A. Tang (in preparation).
42. G. Altarelli, in "Physics at LEP," CERN 68-02.